Cement and Concrete Research 41 (2011) 847–853

Contents lists available at ScienceDirect

Cement and Concrete Research

journal homepage: http://ees.elsevier.com/CEMCON/default.asp

Structural investigation relating to the cementitious activity of bauxite residue — Red mud

Xiaoming Liu [a,*], Na Zhang [b], Henghu Sun [c], Jixiu Zhang [b], Longtu Li [b]

[a] Key Lab of Ecological and Recycle Metallurgy of Chinese Ministry of Education, School of Metallurgical and Ecological Engineering, University of Science and Technology Beijing, Beijing 100083, China
[b] State Key Lab of New Ceramics and Fine Processing, Department of Materials Science and Engineering, Tsinghua University, Beijing 100084, China
[c] School of Engineering and Computer Science, University of the Pacific, Stockton, CA 95211, USA

ARTICLE INFO

Article history:
Received 7 August 2010
Accepted 12 April 2011

Keywords:
Thermal treatment (A)
X-ray diffraction (B)
Spectroscopy (B)
Ca_2SiO_4 (D)
Red mud

ABSTRACT

The cementitious behavior of red mud derived from Bauxite-Calcination method was investigated in this research. Red mud were calcined in the interval 400–900 °C to enhance their pozzolanic activity and then characterized in depth through XRD, FTIR and ^{29}Si MAS-NMR techniques with the aim to correlate phase transitions and structural features with the cementitious activity. The cementitious activity of calcined red mud was evaluated through testing the compressive strength of blended cement mortars. The results indicate that red mud calcined at 600 °C has good cementitious activity due to the formation of poorly-crystallized Ca_2SiO_4. The poorly-crystallized Ca_2SiO_4 is a metastable phase which will transform into highly-crystallized Ca_2SiO_4 with the increase of calcination temperature from 700 °C moving to 900 °C. It is the metastable phase that mainly contributes to the good cementitious activity of red mud. This paper points out another promising direction for the proper utilization of red mud.

1. Introduction

Red mud is an alkaline leaching waste with pH typically 10–12.5. It is generated during Bayer process or Bauxite-Calcination method for alumina production. The disposal of red mud has caused serious environmental problems due to its high alkaline content (Na_2O 2.0–6.0%). Red mud contains major oxides of CaO, SiO_2, Fe_2O_3, Al_2O_3, TiO_2 and Na_2O, and it can be used as an additive to cement, resulting in a good potential for the utilization of red mud in large quantities. The chemical and mineralogical compositions of red muds all over the world are widely different depending on the sources of bauxite, the technological process (Bayer process or Bauxite-Calcination method) and storing ages. However, as a main constitute, iron oxide is generally occurring in red mud, and it is distributed in mineral phases of hematite (Fe_2O_3) or/and goethite (FeOOH). These iron phases mainly control the color and settling properties of red muds [1]. Goethite can be transformed into hematite during a high-temperature calcination process, accompanying with the reinforcement of red color and increase of settling rate [1]. As source of iron oxide, red mud has been investigated in the production of special iron rich cement clinkers [2], or been used as a pozzolanic pigment for colored concrete [3].

Recently, replacing clinker by pozzolanic materials and using new alternative binders produced by industrial solid wastes have become a prime interest in cement industry with attempts to lower CO_2 emissions and decrease the production cost of cement. Some materials with good pozzolanic properties such as fly ash and slag can be utilized directly without heat treatment for the production of blended cement [4–7]. Whereas for other materials such as coal gangue and red mud, their aluminosilicate minerals are expected to be partially destructed and become less crystalline at a relatively higher temperature, so that their pozzolanic properties could be enhanced before being used for the preparation of blended cement [8–10]. Zhang et al. [11] investigated the correlation between silicate polymerization and cementitious activity of coal gangue calcined at different temperatures, and it has been found that phase transitions of clay minerals caused the silicate polymerization degree of coal gangue to change with the increase of temperature, and coal gangue calcined at 600 °C had good pozzolanic property due to the decomposition products of clay materials to form active silica and alumina. Several papers [12–16] have been written on the characterization of red mud through heat treatment. Sglavo et al. [12] carried out a detailed investigation on the thermal behavior of red mud, including phase transformations of the red mud sintered in air for 8 h within the interval 300–1400 °C. Srikanth et al. [13] studied the phase constitution during sintering of pure red mud and red mud–fly ash mixtures in the temperature range of 900–1250 °C. Jobbagy et al. [14] reported the dependence of radon emanation of red mud and red mud–sawdust on heat treatment in the temperature range of 100–1000 °C. Zhang and

* Corresponding author at: Room 810, Yejin Shengtai Building, University of Science and Technology Beijing, Beijing 100083, China. Tel.: +86 10 62332786; fax: +86 10 62333893.
E-mail address: liuxm@ustb.edu.cn (X. Liu).

0008-8846/$ – see front matter © 2011 Elsevier Ltd. All rights reserved.
doi:10.1016/j.cemconres.2011.04.004

Pan [15] made an investigation on the physicochemical characteristics of red mud thermally treated at different temperatures (ambient, 600–900 °C). However, most of the above reports on the characterization of red mud have not investigated the dependence of cementitious activity of red mud on heat treatment. Although Chen et al. [16] simply investigated the properties of red mud heated at 450, 600 and 800 °C and reported that the coordination of Al transformed from 4 to 6 in the red mud heated at 800 °C, the correlation between structure change and cementitious activity of red mud calcined at different temperatures has not been figured out.

In the present work, the cementitious behavior of Bauxite-Calcination-method red mud calcined within the interval 400–900 °C has been investigated. The aim was to correlate solid-state phase transitions and structural features deduced from TG–DTA, XRD, FTIR and ^{29}Si MAS-NMR techniques with the cementitious activity of red mud calcined at different temperatures. The cementitious activity of calcined red mud was evaluated by means of testing the compressive strength of blended cement mortars. This work provides an important base for a long-term project on the utilization of red mud in cement industry.

2. Materials and experimental methods

2.1. Materials

Red mud samples with age of 3 years old were obtained from Shandong alumina refining plant, the process of which is Bauxite-Calcination method. Ordinary Portland cement clinker from Beijing Xingang Cement Plant was used in this experiment, and its mineralogical phases are presented in Fig. 1. The chemical compositions of the red mud on dry basis (dried at 100 °C) and clinker determined by X-ray fluorescence (XRF-1700) analyzer are given in Table 1.

2.2. Experimental procedure

The red mud was dried in an oven and ground down by using a ball mill. The size distribution of the ground red mud particles obtained from a laser diffraction particle size analyzer is shown in Fig. 2. It can be seen that the ground red mud particles are mostly within the range of 3–70 μm with a mean of 23.2 μm. To decide an adequate calcination temperature, at which the aluminosilicate materials composed in the red mud are expected to be partially destructed and become less crystalline, thermal analysis of the dried red mud was performed on a Netzsch STA 449 C Thermal analyzer. TG–DTA analysis was performed in the range of 80–1050 °C (stripping gas: dry N_2 and heating rate: 10 °C/min).

Powder batches (about 400 g red mud for each batch) were calcined for lasting 3 h in a programmable electrical furnace at 400, 500, 600, 700, 800 and 900 °C. The calcined red mud samples were removed from the furnace and allowed to cool spontaneously to room temperature in air.

X-ray diffraction (XRD) analysis of the red mud samples at different calcination temperatures were carried out with Rigaku D/max-RB X-ray diffractometer using CuKα radiation, voltage 40 kV, current 200 mA and 2θ scanning, ranging between 5° and 70°.

SEM observation was carried out on JSM-6460LV scanning electron microscope for examination of micromorphological characteristics of red mud calcined at 600 °C.

Infrared spectra of the red mud treated at different temperatures were recorded on a Spectrum GX Perkin-Elmer Fourier transform infrared (FTIR) spectrometer using the KBr pellet technique.

^{29}Si solid-state magic-angle spinning (MAS) nuclear magnetic resonance (NMR) spectroscopy was carried out using a BRUKER-AM300 spectrometer (Germany) operating at 59.62 MHz for the ^{29}Si resonance frequencies.

Table 1
Chemical composition of dried red mud and clinker.

Oxides (%)	Red mud	Clinker
CaO	35.09	66.09
SiO_2	18	21.94
Al_2O_3	6.31	5.27
Fe_2O_3	12.38	2.96
Na_2O	2.71	0.3
K_2O	0.45	0.7
MgO	1.13	0.88
TiO_2	3.32	–
SO_3	0.54	0.31
LOI	20.07	0.67

3. Results and discussion

3.1. TG–DTA analysis

The TG–DTA diagram of dried red mud is given in Fig. 3. It shows two major steps for the mass loss with the change in temperature. The first step occurred in the range of 80–500 °C corresponding to the physically absorbed water and chemically bound water. As the red

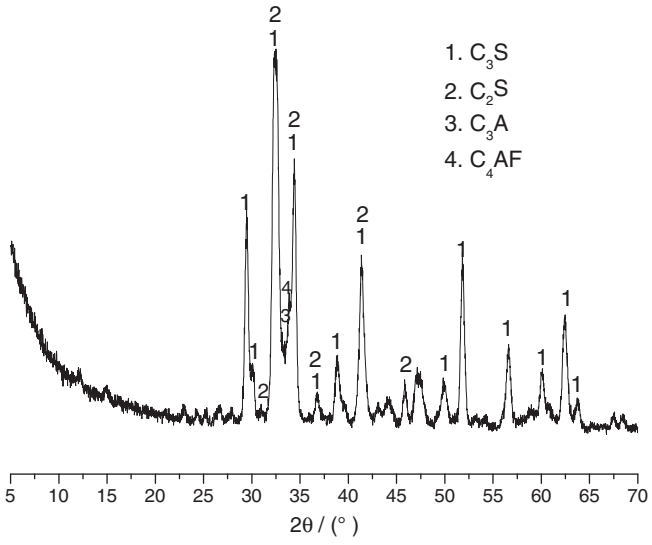

Fig. 1. Mineralogical phases of clinker.

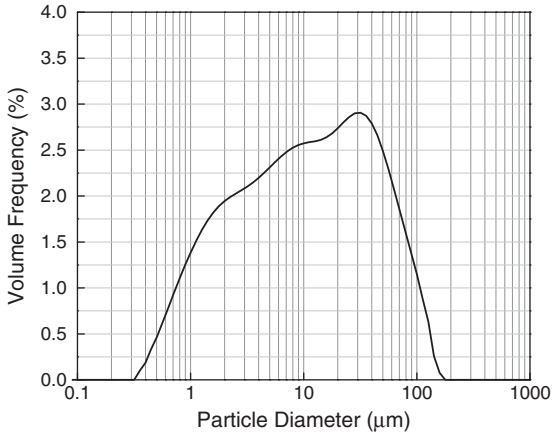

Fig. 2. Particle size distribution of red mud obtained from a laser diffraction particle size analyzer.

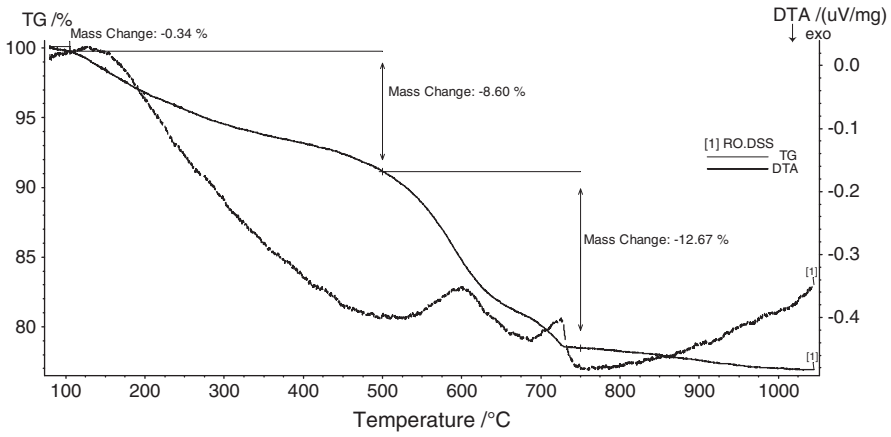

Fig. 3. TG–DTA diagram of dried red mud.

mud sample had been dried at 100 °C when it was used for thermogravimetric analysis, most of the physically absorbed water dissipated in the drying process, and therefore the physically absorbed water tested in the TGA diagram was about 0.34% of the total weight corresponding to the temperature range of 80–105 °C. The temperature range of 105–500 °C with mass loss of 8.6% of the total weight was mainly related to the evaporation of chemically bound water. The second step with significant mass loss of 12.67% of the total weight can be detected in the range of 500–750 °C, most likely to be corresponding to the release of CO_2 during the decomposition of carbonates. It is notable that two endothermic peaks (around 600 °C and 725 °C) occurred within the interval 500–750 °C, suggesting two carbonate phases present in the red mud sample.

3.2. XRD analysis

The elemental analysis and phase characterization of red mud derived from bauxites have been investigated by several researchers [3,12,13,15–17]. However, red mud is a complex industrial waste, and its chemical composition and mineralogical phases vary widely all over the world. The chemical analysis of red mud used in this study indicates predominantly the presence of calcium, silicon, iron and aluminum, and small amounts of titanium and sodium. The XRD patterns of the red mud uncalcined and calcined within the interval 400–900 °C are shown in Fig. 4. It can be seen that the major phases present in the uncalcined red mud are calcite ($CaCO_3$), aragonite ($CaCO_3$), Ca_2SiO_4, perovskite ($CaTiO_3$), hematite (Fe_2O_3), and gibbsite ($Al(OH)_3$). Perovskite and hematite are not affected by the heating treatment up to 900 °C. Gibbsite cannot be detected in the sample treated at 400 °C, neither crystalline Al_2O_3 is detected within the temperature interval 400–900 °C. According to the observation made by Sglavo et al. [12], it is thought that gibbsite ($Al(OH)_3$ phase) here considered decomposes to reactive aluminum oxide at 400 °C, the crystallinity and stability of which are much lower than those of corundum (α-Al_2O_3). $CaCO_3$ phases are present in aragonite and calcite. It is noted that with the increase of temperature up to 600 °C, the peaks of aragonite diminish and they even completely collapse at 600 °C. Meanwhile, CaO can be detected in samples treated at 500 and 600 °C. This suggests the decomposition of aragonite to CaO in the interval 500–600 °C. Calcite can be detected within the range of 400–700 °C. However, it is observed that the peaks of calcite diminish obviously at 700 °C and eventually disappear at 800 °C, suggesting the decomposition of calcite into CaO in the interval 700–800 °C. These results are consistent with the above TG–DTA analysis.

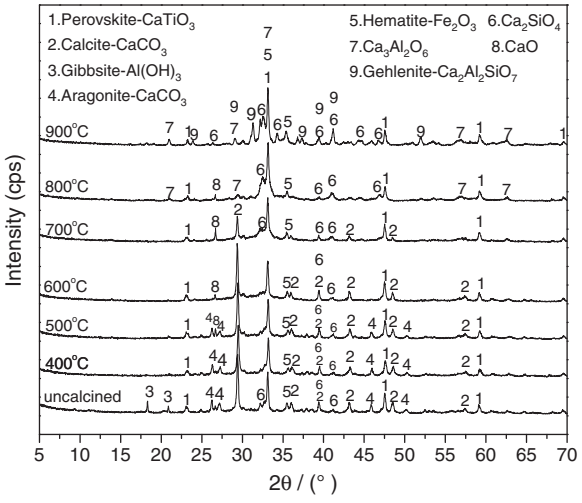

Fig. 4. XRD patterns of red mud uncalcined and calcined at different temperatures.

Ca_2SiO_4 phase is present in the raw red mud used in this work. In alumina production by using Bauxite-Calcination method, bauxite ores are generally mixed with sodium carbonate and limestone, and the mixtures are sintered under high temperature [17]. Due to most of local bauxite ores in China contain a high portion of silicon, Ca_2SiO_4 can be formed in the calcination process (above 1200 °C) and subsequently present in the bauxite calcination residue — red mud. Ca_2SiO_4 constitutes the fundamental phase in the investigated temperature interval 400–900 °C. It is interesting to notice that the peaks of Ca_2SiO_4 increase gradually from 700 up to 900 °C, indicating the formation of crystallized Ca_2SiO_4. Moreover, $Ca_3Al_2O_6$ phase is detected in specimen treated at 800 and 900 °C, and gehlenite ($Ca_2Al_2SiO_7$) appears in the red mud calcined at 900 °C.

The main peaks of Ca_2SiO_4 in the red mud uncalcined and calcined within the interval 400–900 °C are shown in Fig. 5 with an attempt to obtain more detailed information about Ca_2SiO_4. The peaks of Ca_2SiO_4 are similar in the XRD patterns of red mud uncalcined and calcined at 400 and 500 °C. However, it is found that the peaks of Ca_2SiO_4 are very obscure at 600 °C, suggesting poorly-crystallized Ca_2SiO_4 occurring in the red mud calcined at 600 °C. Combining the SEM photograph of red mud sample calcined at 600 °C (see Fig. 6), it is observed that the particles of red mud at 600 °C were in poorly-crystallized or amorphous forms. This indicates that the red mud calcined at 600 °C may be more reactive than those calcined at other temperatures, and may provide good cementitious property when used for blended cement.

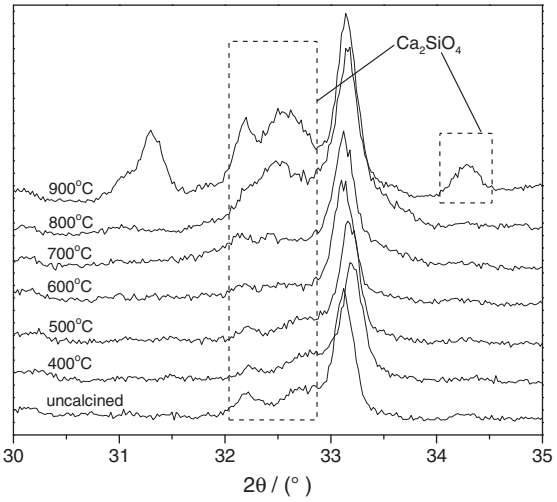

Fig. 5. XRD patterns of Ca_2SiO_4 in the red mud uncalcined and calcined at different temperatures.

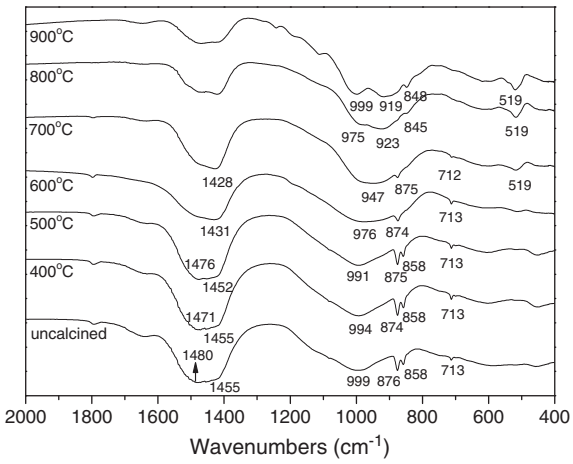

Fig. 7. FTIR spectra of red mud uncalcined and calcined at different temperatures.

3.3. FTIR analysis

Fig. 7 displays infrared spectra of red mud uncalcined and calcined within the interval 400–900 °C, respectively. The results concerning main phases identified by FTIR analysis are summarized in Table 2.

Infrared spectra of the red mud uncalcined and calcined at 400 and 500 °C are rather similar, presenting analogous absorption bands. The bands around 1471–1480 cm^{-1}, and small shoulders at 858 cm^{-1}, respectively, are related to anti-symmetric C–O stretching (υ_3) vibrations and out-of-plane C–O bending (υ_2) vibrations in CO_3^{2-} ions of aragonite. However, these bands disappear in the infrared spectra of red mud calcined at 600 °C and above 600 °C. This provides remarkably good correspondence with the XRD analysis, suggesting the decomposition of aragonite between 500 and 600 °C.

Infrared spectra of all samples with the exception of red mud calcined at 800 and 900 °C show bands around 1428–1455 cm^{-1}, 874–876 cm^{-1} and 712–713 cm^{-1}, respectively, associated with anti-symmetric stretching (υ_3), out-of-plane bending (υ_2) and in-plane bending (υ_4) modes of CO_3^{2-} ions of calcite [18–21]. It is observed that these bands due to calcite decline with the increasing temperature and they almost completely disappear when red mud calcined at 800 °C, which confirms the XRD results and indicates that most of calcite in red mud decomposes yielding CaO before 800 °C.

All spectra show bands in the range of 919–999 cm^{-1} corresponding to anti-symmetric Si–O stretching vibrations (υ_3) in SiO_4 tetrahedra of Ca_2SiO_4 [18,19,21–24]. In IR spectra of red mud calcined at 700, 800 and 900 °C, a shoulder at 519 cm^{-1} ascribed to out-of-plane O–Si–O bending modes (υ_4) in SiO_4 tetrahedra of Ca_2SiO_4 [19,21,24] was detected. It is also noted that the intensity of this observed band (519 cm^{-1}) increases with the calcination temperature up to 900 °C, suggesting more and more Ca_2SiO_4 formed when the red mud calcined from 700 to 900 °C. Meanwhile, the absorption band at 947 cm^{-1} (in the spectra of 700 °C) was split into two bands around 975 and 923 cm^{-1} (in the spectra of 800 °C), and two sharper bands at 999 and 919 cm^{-1} (in the spectra of 900 °C), indicative of the formation of more highly crystallized Ca_2SiO_4 with the increase of temperature from 700 to 900 °C. In addition, two new bands at 845 and 848 cm^{-1} appearing respectively in the IR spectra of red mud calcined at 800 and 900 °C can be related to symmetric Si–O stretching vibrations (υ_1) in SiO_4 tetrahedra of Ca_2SiO_4 [24], suggesting that the Ca_2SiO_4 formed in the red mud calcined at 800 and 900 °C has highly symmetrical characteristic.

Combining the FTIR analysis with the results of TG–TDA and XRD, possible solid state reactions in the 400–900 °C interval can be deduced: (1) at 400 °C, the dehydration of gibbsite yielding reactive Al_2O_3: $2Al(OH)_3 \rightarrow Al_2O_3 + 3H_2O$, (2) 500–600 °C, the decomposition of aragonite: $CaCO_3 \rightarrow CaO + CO_2$, (3) at 600 °C, the formation of poorly-crystallized Ca_2SiO_4; (4) 700–800 °C, the decomposition of calcite: $CaCO_3 \rightarrow CaO + CO_2$, (5) 700–900 °C, the formation of highly-crystallized Ca_2SiO_4 with the increase of calcination temperature, (6) 800–900 °C, the formation of $Ca_3Al_2O_6$ from CaO and reactive Al_2O_3: $3CaO + Al_2O_3 \rightarrow Ca_3Al_2O_6$, and (7) at 900 °C, the formation of gehlenite from CaO, reactive Al_2O_3 and reactive SiO_2: $2CaO + Al_2O_3 + SiO_2 \rightarrow Ca_2Al_2SiO_7$.

Combining the TG data and chemical composition of red mud with the phases of $Al(OH)_3$, $CaCO_3$ and Ca_2SiO_4, more valuable information can be obtained. Based on the CO_2 loss (12.67%) recorded by TG, the amount of $CaCO_3$ in the red mud was calculated to be 28.80%, and the amount of CaO fixed in $CaCO_3$ would be 16.13%. Considering that

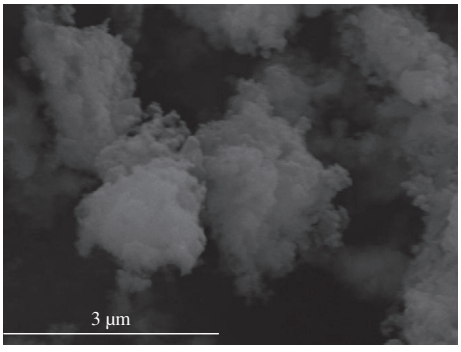

Fig. 6. SEM photograph of red mud calcined at 600 °C.

Table 2
The main corresponding phases determined by FTIR for red mud uncalcined and calcined at different temperatures.

Wavenumbers/cm^{-1}							Phases
Uncalcined	400 °C	500 °C	600 °C	700 °C	800 °C	900 °C	
1480	1471	1476	–	–	–	–	Aragonite
1455	1455	1452	1431	1428	–	–	Calcite
999	994	991	976	947	975	999	Ca_2SiO_4
876	874	875	874	875	–	–	Calcite
858	858	858	–	–	–	–	Aragonite
713	713	713	713	712	–	–	Calcite
–	–	–	–	519	519	519	Ca_2SiO_4
–	–	–	–	–	845	848	Ca_2SiO_4
–	–	–	–	–	923	919	Ca_2SiO_4

35.09% CaO was contained in the red mud as seen in Table 1, the amount of CaO not fixed as $CaCO_3$ would be 18.96%. As shown in Table 1, the content of Al_2O_3 in the red mud was 6.31%. If considering that 6.31% of Al_2O_3 was fixed as $Al(OH)_3$, the mass loss due to the decomposition of $Al(OH)_3$ would be 3.34%. However, the mass loss during 105–500 °C is 8.6% according to the TG analysis, which suggests that there is another phase in the red mud losing water before 500 °C. Furthermore, it can be seen from Table 1 that the content of SiO_2 in the original red mud sample was 18%, but Fig. 4 displays that the uncalcined red mud contain a small amount of Ca_2SiO_4, which indicates that an amorphous phase containing SiO_2 could be occurring in the raw red mud. Liu et al. [17] reported there were about 20% of amorphous materials in the red mud derived from a combined Bayer process and Bauxite-Calcination method. Through TEM observation, Zhang and Pan [15] also found that there were certain amounts of amorphous aluminosilicates contained in the red mud derived from Bauxite-Calcination method, the source of which was the same with the red mud we used in the present work. Therefore, it is thought that amorphous aluminosilicates could be occurring in the red mud specimen used in this experiment, and these amorphous aluminosilicates might decompose yielding reactive alumina and silica with the increase of calcination temperature, which would be involved in the formation of Ca_2SiO_4, $Ca_3Al_2O_6$ and $Ca_2Al_2SiO_7$.

3.4. Evaluation of cementitious activity by compressive strength test

In order to find out an optimum calcination temperature under which the red mud would have good cementitious reactivity, compressive strength of blended cement mortars at 3, 7 and 28 days was tested according to Chinese Standard GB/T17671-1999 [25]. The blended cement was composed of 50% red mud, 45% clinker and 5% gypsum. Fig. 8 displays the compressive strength results as a function of calcination temperature. The compressive strength values (at 3, 7 and 28 days) of blended cement mortars changed with the calcination temperature. It can be safely stated that calcination temperature has a significant effect on the cementitious behavior of red mud. According to the test results, the best 28-day compressive strength value of 34.15 MPa was obtained by blended cement produced with red mud calcined at 600 °C. This confirms the result of XRD analysis that red mud calcined at 600 °C has good cementitious activity due to the formation of poorly-crystallized Ca_2SiO_4. Although the amounts of Ca_2SiO_4 and $Ca_3Al_2O_6$ occurring in the red mud calcined at 900 °C were higher than those present in the red mud calcined at 800 °C, the compressive strength values (at 3, 7 and 28 days) of red mud calcined at 900 °C were slightly lower than those at 800 °C. This can be explained from two viewpoints: (1) the formation of gehlenite ($Ca_2Al_2SiO_7$) has an unfavorable effect on the cementitious behavior of red mud calcined at 900 °C, and (2) Ca_2SiO_4 formed in the red mud calcined at 900 °C has higher crystallized and symmetrical structure resulting in the decline of compressive strength.

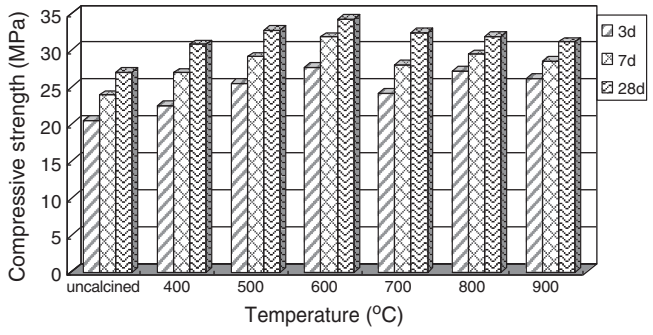

Fig. 8. Compressive strength of red mud blended cement mortars versus calcination temperature.

3.5. ^{29}Si MAS-NMR analysis

^{29}Si MAS-NMR appears as a powerful technique to probe structure features of crystalline and poorly crystalline or amorphous phases. It can distinguish the different SiQ^n structural units in aluminosilicates. In order to get an insight into the changes of structural units in red mud during calcination, ^{29}Si MAS-NMR was performed particularly on the uncalcined red mud, and samples at 600 and 900 °C.

Fig. 9 shows the ^{29}Si MAS-NMR spectra for the red mud uncalcined and calcined at 600 and 900 °C, respectively. Two major environments can be deduced from the ^{29}Si NMR spectrum of uncalcined red mud. One centered at −80 ppm is associated to SiQ^1 unit (disilicates or chain end groups), and the other at −70 ppm is related to SiQ^0 unit (orthosilicates). From the XRD pattern of uncalcined red mud (shown in Fig. 4), no aluminosilicate phases were detected except Ca_2SiO_4. It is known that the SiQ^0 unit is arising from Ca_2SiO_4 in the initial red mud. While for the left major content of SiQ^1 unit, where is it from? According to the discussion in the Section 3.3, certain amounts of

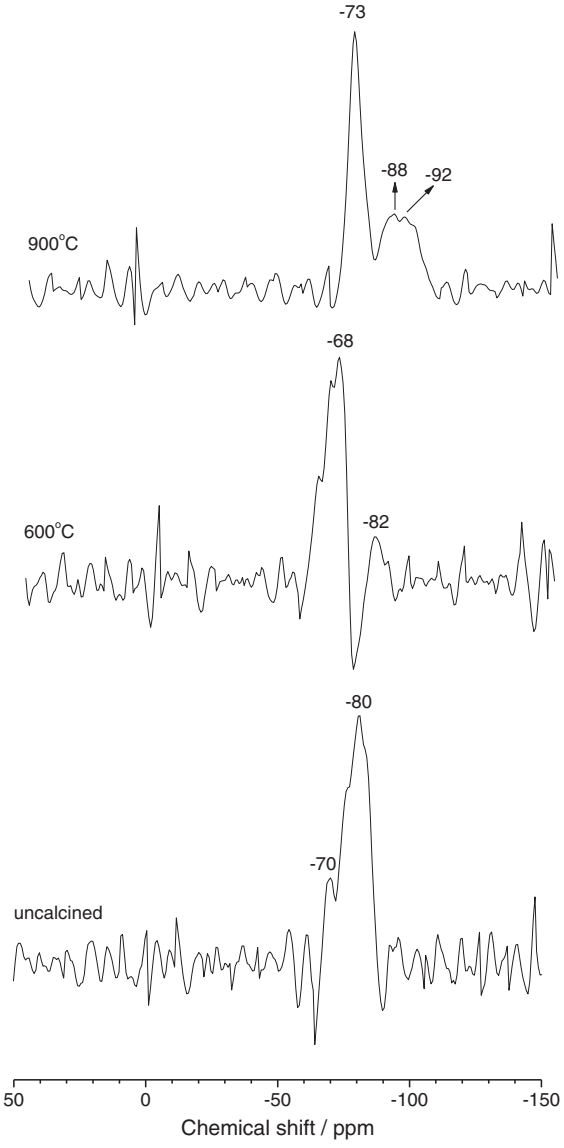

Fig. 9. ^{29}Si MAS-NMR spectra of red mud uncalcined and calcined at 600 and 900 °C.

amorphous aluminosilicates were thought to be contained in the red mud derived from Bauxite-Calcination method. Amorphous phase is generally hard to be detected by XRD technique, but it can be figured out through MAS-NMR analysis. The ^{29}Si MAS-NMR spectrum for the uncalcined red mud proves that, except with small amount of Ca_2SiO_4, most of the siliceous materials are presented as SiQ^1 unit arising from amorphous aluminosilicates.

^{29}Si NMR spectrum of red mud calcined at 600 °C shows significant differences from that of uncalcined red mud. It displays a major peak at −68 ppm originating from SiQ^0 unit and a negligibly smaller one at −82 ppm related to SiQ^1 unit. Compared to the uncalcined red mud, the general characteristic of the spectrum for the red mud calcined at 600 °C is a significant increase of SiQ^0 unit accompanying with a decrease of SiQ^1 unit, which reflects that SiQ^1 unit transforms to SiQ^0 unit with the increase of calcination temperature up to 600 °C. It indicates that most of the siliceous materials are presented as SiQ^0 unit in the red mud calcined at 600 °C. From this point of view, it is believed that large amounts of poorly-crystallized Ca_2SiO_4 have been formed at 600 °C resulting from the decomposition of amorphous aluminosilicates.

^{29}Si NMR spectrum of red mud calcined at 900 °C is very different from both of the above spectra. It shows a major content of SiQ^0 unit in connection with a sharper peak centered at −73 ppm, indicative of the highly-crystallized Ca_2SiO_4. In addition, it displays two bands at −92 and −88 ppm assigned to SiQ^3 and SiQ^3(1Al) units, respectively. According to the XRD pattern of red mud calcined at 900 °C (shown in Fig. 4), Si is presented in phases of Ca_2SiO_4 and $Ca_2Al_2SiO_7$ (gehlenite). It is obvious that Ca_2SiO_4 has the orthosilicate structure of SiQ^0 unit, so is it possible that the observed SiQ^3 and SiQ^3(1Al) units correspond to gehlenite? In the literature [26], it is reported that akermanite ($Ca_2MgSi_2O_7$) has a ^{29}Si NMR chemical shift at −73.9 ppm related to SiQ^1 unit. However, there is little information reported for the ^{29}Si NMR chemical shifts of $Ca_2Al_2SiO_7$. Gehlenite is a single layer silicate, and its structure [27] is shown in Fig. 10. In each unit cell, the two tetrahedrally coordinated T_1 sites are always occupied by Al atoms, whereas the four tetrahedral T_2 sites are disordered, with equal numbers of Al and Si atoms distributed on them [28]. As shown in Fig. 10, the T_2 sites are grouped into pairs. There is no nearest neighboring T_2-O-T_2 linkage between pairs, but T_2-O-T_2 pairs are connected through the linkage of T_1 sites to form a single layer structure. Each T_2 tetrahedron has three bridging oxygen and an apical oxygen. Due to the T_2 sites that are disordered, T_2-O-T_2 pairs could be in forms of Si–O–Al or Si–O–Si. Thus, it is thought that structural unit of SiQ^3 occurs when T_2-O-T_2 pairs presenting as Si–O–Si form, and SiQ^3(1Al) unit appears when T_2-O-T_2 pairs presenting as Si–O–Al form. This interpretation is perfectly consistent with the above ^{29}Si NMR analysis for the bands at −92 and −88 ppm, suggesting that gehlenite formed in the red mud calcined at 900 °C has structural units of SiQ^3 and SiQ^3(1Al). It is this highly polymerized structure arising from $Ca_2Al_2SiO_7$ observed in the present study that plays unfavorable effect on the cementitious activity of red mud calcined at 900 °C.

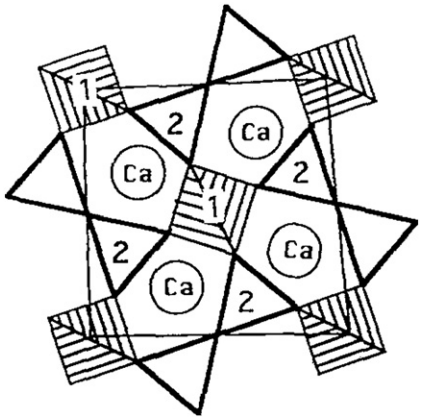

Fig. 10. The unit cell of gehlenite ($Ca_2Al_2SiO_7$) structure [24]. 1 and 2 marked represent T_1 and T_2 tetrahedra, which are two distinct tetrahedral sites.

Comparison among ^{29}Si MAS-NMR spectra of uncalcined red mud and red mud calcined at 600 and 900 °C shows that the red mud calcined at 600 °C is mainly composed of SiQ^0 unit corresponding to poorly-crystallized Ca_2SiO_4. Combining the results of XRD and FTIR analysis, it is concluded that the poorly-crystallized Ca_2SiO_4 present in the red mud at 600 °C is a new formed phase by reaction $2CaO + SiO_2 \rightarrow Ca_2SiO_4$, in which the reactive SiO_2 is derived from the decomposition of amorphous aluminosilicates. The poorly-crystallized Ca_2SiO_4 is a metastable phase which will transform into highly-crystallized Ca_2SiO_4 with the increase of calcination temperature from 700 moving to 900 °C. It is the metastable phase that mainly contributes to the good cementitious activity of red mud at 600 °C.

4. Conclusions

An in-depth characterization of red mud has been performed to investigate the phase transitions and structural features in relation to cementitious activity during calcination within the interval 400–900 °C. This study provides an incisive understanding for the cementitious behavior of red mud derived from Bauxite-Calcination method.

The major phases present in the raw red mud are calcite ($CaCO_3$), aragonite ($CaCO_3$), Ca_2SiO_4, perovskite ($CaTiO_3$), hematite (Fe_2O_3), and gibbsite ($Al(OH)_3$). Perovskite and hematite are not affected by the heat treatment up to 900 °C. The solid state reactions in the interval 400–900 °C can be deduced: (1) at 400 °C, the dehydration of gibbsite yielding reactive Al_2O_3, (2) 500–600 °C, the decomposition of aragonite, (3) at 600 °C, the formation of poorly-crystallized Ca_2SiO_4, (4) 700–800 °C, the decomposition of calcite, (5) 700–900 °C, the formation of highly-crystallized Ca_2SiO_4, (6) 800–900 °C, the formation of $Ca_3Al_2O_6$, and (7) at 900 °C, the formation of gehlenite ($Ca_2Al_2SiO_7$).

Calcination temperature has a significant effect on the cementitious activity of red mud due to the phase transitions during the calcination process. It is found that red mud calcined at 600 °C in this study had the best cementitious activity due to the formation of poorly-crystallized Ca_2SiO_4. With the increase of calcination temperature from 700 to 900 °C, more and more Ca_2SiO_4 formed in the calcined red mud samples, and the crystallinity of Ca_2SiO_4 also increased.

^{29}Si MAS-NMR spectroscopy has shown progressive structural changes from the red mud uncalcined to the red mud calcined at 900 °C: SiQ^1 and SiQ^0 units (uncalcined sample) to major content of SiQ^0 unit (sample at 600 °C) and finally to SiQ^0, SiQ^3 and SiQ^3(1Al) units (sample at 900 °C). Combining the results of XRD, FTIR and ^{29}Si MAS-NMR analysis, it is concluded that the poorly-crystallized Ca_2SiO_4 present in the red mud at 600 °C is a new formed phase by reaction $2CaO + SiO_2 \rightarrow Ca_2SiO_4$, in which the reactive SiO_2 is derived from the decomposition of amorphous aluminosilicates. The poorly-crystallized Ca_2SiO_4 is a metastable phase which will transform into highly-crystallized Ca_2SiO_4 with the increase of calcination temperature from 700 moving to 900 °C. It is the metastable phase that mainly contributes to the good cementitious activity of red mud at 600 °C.

This study provides a fundamental point for the use of red mud as clinker replacement for the production of blended cement, which points out another promising direction for the proper utilization of red mud in large quantities. It is economically viable to perform a 600 °C calcination of red mud to improve its cementitious properties, and using the subsequent red mud to develop blended cement not

only can help to mitigate environmental pollution, but also can save a lot of natural resources for the cement clinker.

Acknowledgments

This work has been financially supported by the National Natural Science Foundation of China (NSFC, NO. 50674062 and NO. 51034008) and China Postdoctoral Science Foundation funded project (20100480202). The authors gratefully acknowledge Analytical and Testing Center of Tsinghua University for supplying synthesis facilities to carry out this research work.

References

[1] L.Y. Li, A study of iron mineral transformation to reduce red mud tailings, Waste Manage 21 (2001) 525–534.
[2] M. Singh, S.N. Upadhayay, P.M. Prasad, Preparation of iron rich cements using red mud, Cem. Concr. Res. 27 (1997) 1037–1046.
[3] J. Pera, R. Boumaza, J. Ambroise, Development of a pozzolanic pigment from red mud, Cem. Concr. Res. 27 (1997) 1513–1522.
[4] M. Singh, M. Garg, Cementitious binder from fly ash and other industrial wastes, Cem. Concr. Res. 29 (1999) 309–314.
[5] Z. Li, Z. Ding, Property improvement of Portland cement by incorporating with metakaolin and slag, Cem. Concr. Res. 33 (2003) 579–584.
[6] M.S. Konsta-Gdoutos, S.P. Shah, Hydration and properties of novel blended cements based on cement kiln dust and blast furnace slag, Cem. Concr. Res. 33 (2003) 1269–1276.
[7] K. Luke, E. Lachowski, Internal composition of 20-year-old fly ash and slag-blended ordinary Portland cement pastes, J. Am. Ceram. Soc. 91 (2008) 4084–4092.
[8] N. Zhang, H. Sun, X. Liu, J. Zhang, Early-age characteristics of red mud–coal gangue cementitious material, J. Hazard. Mater. 167 (2009) 927–932.
[9] D. Li, X. Song, C. Gong, Z. Pan, Research on cementitious behavior and mechanism of pozzolanic cement with coal gangue, Cem. Concr. Res. 36 (2006) 1752–1759.
[10] H. Li, H. Sun, X. Xiao, H. Chen, Mechanical properties of gangue-containing aluminosilicate based cementitious materials, J. Univ. Sci. Technol. B 13 (2006) 183–189.
[11] J. Zhang, H. Sun, Y. Sun, N. Zhang, Correlation between ^{29}Si polymerization and cementitious activity of coal gangue, J. Zhejiang Univ. Sci. A 10 (2009) 1334–1340.
[12] V.M. Sglavo, R. Campostrini, S. Maurina, G. Carturan, M. Monagheddu, G. Budroni, G. Cocco, Bauxite 'red mud' in the ceramic industry. Part 1: thermal behavior, J. Eur. Ceram. Soc. 20 (2000) 235–244.
[13] S. Srikanth, A.K. Ray, A. Bandopadhyay, B. Ravikumar, Phase constitution during sintering of red mud and red mud–fly ash mixtures, J. Am. Ceram. Soc. 88 (2005) 2396–2401.
[14] V. Jobbagy, J. Somlai, J. Kovacs, G. Szeiler, T. Kovacs, Dependence of radon emanation of red mud bauxite processing wastes on heat treatment, J. Hazard. Mater. 172 (2009) 1258–1263.
[15] Y. Zhang, Z. Pan, Characterization of red mud thermally treated at different temperatures, J. Jinan Univ. Sci. Tech. 19 (2005) 293–297 (in Chinese).
[16] H. Chen, H. Sun, H. Li, Effect of heat treatment temperature on cementitious activity of red mud, Light Metals 9 (2006) 22–25 (in Chinese).
[17] Y. Liu, C. Lin, Y. Wu, Characterization of red mud derived from a combined Bayer Process and bauxite calcination method, J. Hazard. Mater. 146 (2007) 255–261.
[18] P. Yu, R.J. Kirkpatrick, B. Poe, P.F. McMillan, X. Cong, Structure of calcium silicate hydrate (C-S-H): near-, mid-, and far-infrared spectroscopy, J. Am. Ceram. Soc. 82 (1999) 742–748.
[19] I. Lecomte, C. Henrist, M. Liegeois, F. Maseri, A. Rulmont, R. Cloots, (Micro)-structure comparison between geopolymers, alkali-activated slag cement and Portland cement, J. Eur. Ceram. Soc. 26 (2006) 3789–3797.
[20] C. Li, H. Sun, Z. Yi, L. Li, Innovative methodology for comprehensive utilization of iron ore tailings Part 2: the residues after iron recovery from iron ore tailings to prepare cementitious material, J. Hazard. Mater. 174 (2010) 78–83.
[21] A. Fernandez-Jimenez, F. Puertas, I. Sobrados, J. Sanz, Structure of calcium silicate hydrates formed in alkaline-activated slag: influence of the type of alkaline activator, J. Am. Ceram. Soc. 86 (2003) 1389–1394.
[22] A. Fernandez-Jimenez, A. Palomo, T. Vazquez, R. Vallepu, T. Terai, K. Ikeda, Alkaline activation of blends of metakaolin and calcium aluminate cement. Part I: strength and microstructural development, J. Am. Ceram. Soc. 91 (2007) 1231–1236.
[23] Z. Yi, Research on the formation mechanism and application of cementitious activity of iron ore tailings, Dissertation of Doctoral Degree, Beijing: Tsinghua University, 2009, p.61.
[24] J. Besnsted, S.P. Varma, Some application of infra-red and Raman spectroscopy in cement chemistry part 1 — examination of dicalcium silicate, Cement Technol. 5 (1974) 256–261.
[25] GB/T17671-1999. Test method for cements — determination of strength.
[26] N. Janes, E. Oldfield, Prediction of silicon-29 nuclear magnetic resonance chemical shifts using a group electronegativity approach: applications to silicate and aluminosilicate structures, J. Am. Chem. Soc. 107 (1985) 6769–6775.
[27] S. Thayaparam, M.T. Dove, V. Heine, A computer simulation study of Al/Si ordering in gehlenite and the paradox of the low transition temperature, Phys. Chem. Minerals 21 (1994) 110–116.
[28] M. Kimata, N. Ii, The structural properties of synthetic Gehlenite $Ca_2Al_2SiO_7$, N. Jahrb. Mineral Abh. 144 (1982) 254–267.